

Registration and Nucleation of the $\text{Ag}/\text{Si}(111) (\sqrt{3} \times \sqrt{3})R30^\circ$ Structure by Scanning Tunneling Microscopy

R. J. Wilson and S. Chiang

IBM Almaden Research Center, San Jose, California 95120

(Received 29 June 1987)

Scanning tunneling microscope images showing the lateral registration of the $\text{Ag}/\text{Si}(111) (\sqrt{3} \times \sqrt{3})R30^\circ$ structure relative to the $\text{Si}(111)7 \times 7$ structure demonstrate that protrusions are observed at threefold hollow sites. These protrusions can thus be associated with Ag atoms in the honeycomb structure but not with Si atoms in the embedded-trimer structure. Images of domain boundaries and steps also suggest that the top double layer of Si is intact, in disagreement with another recent model.

PACS numbers: 68.35.Bs

The structure of the $(\sqrt{3} \times \sqrt{3})R30^\circ$, or simply $\sqrt{3}$, $\text{Ag}/\text{Si}(111)$ surface has recently been the subject of considerable controversy. This controversy began when we first reported scanning tunneling microscopy (STM) observations of a honeycomb structure¹ which was consistent with a honeycomb (H) model² based on an array of Ag atoms embedded in threefold hollow sites of the Si surface. Subsequently, van Loenen *et al.*³ presented current-imaging tunneling spectroscopy data showing a honeycomb arrangement of protrusions which they interpreted as top-layer Si atoms of an embedded-trimer (ET) structure.⁴ More recently, Kono *et al.*⁵ exhibited photoemission data which support the honeycomb arrangement of Ag atoms which they believe to be embedded in a missing top-layer (MTL) structure where only the lower half of the $\text{Si}(111)$ double layer is present. These models differ significantly, even in saturation Ag coverage, and can be tested by the establishment of the registration of features observed in STM relative to the surface Si mesh.

In this Letter we present new STM registration data, taken on surfaces where the $\sqrt{3}$ $\text{Ag}/\text{Si}(111)$ structure and the clean $\text{Si}(111)7 \times 7$ structure are simultaneously present, which rule out the ET model, demonstrate the incorrectness of the current-imaging tunneling spectroscopy interpretation, and argue strongly against the MTL model. This novel application of straightforward registration techniques to deduce an unknown surface structure from a known structure in an adjacent domain promises to be an extremely powerful STM technique for the determination of atomic identity and surface structure whenever domain boundaries or adsorbates with known binding sites can be observed.

The present work required the observation of islands of the $\sqrt{3}$ structure which are formed when Ag is deposited onto samples at elevated temperatures.² Our ultrahigh-vacuum STM surface-analysis system⁶ and sample preparation¹ have been modified only in that Ag could be deposited on samples held at 500°C . Deposition of less than 0.1 monolayer onto heated Si samples now allows us to image boundaries between essentially

perfect 7×7 and $\sqrt{3}$ domains, which are readily found at step edges bounding pristine 7×7 terraces.

Once domain boundaries between the 7×7 and $\sqrt{3}$ structures were obtained, the registration of the two structures was determined as follows. First, there is good agreement on the dimer-adatom-stacking-fault (DAS) structure⁷ of the $\text{Si}(111)7 \times 7$ surface which places Si adatoms at threefold hollow sites directly above second-layer Si atoms, as shown in Fig. 1. Secondly, STM images are well studied for this surface,⁸⁻¹⁰ and it is known that the adatom topography is obtained for negative tip bias whereas positive-tip-bias images allow identification of the faulted half-cell.¹⁰ Once the Si adatoms of the 7×7 structure are registered with their known lattice sites, the positions of the honeycomb of protrusions in the STM image of the $\sqrt{3}$ structure with respect to the $\text{Si}(111)$ mesh can be determined. The positions of the protrusions of the $\sqrt{3}$ structure for the H, ET, and MTL models are shown in Fig. 1. It is clear that the positions of the Si protrusions of the ET structure are laterally shifted relative to the Ag protrusions of the H and MTL structures. It is also clear that surface Si atoms occupy different lateral positions in the H and MTL models.

One technical difficulty arises regarding the simultane-

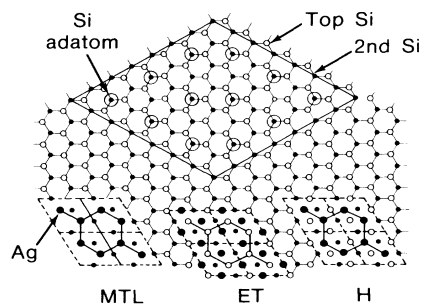


FIG. 1. Adatom positions for the $\text{Si}(111)7 \times 7$ DAS structure (top) and three models for the $\sqrt{3}$ $\text{Ag}/\text{Si}(111)$ surface (bottom).

ous gray-level image display of steps, the 2-Å corrugation of the 7×7 , and the 0.2-Å corrugation of $\sqrt{3}$ regions. These corrugations were observed at tip bias voltages V_T near -2 V and tunnel currents $i_T=2.0$ nA used to obtain the data for Figs. 2-4. We have obtained satisfactory results when image contrast is enhanced by the method of statistical differencing,¹¹ a standard technique in digital image processing. For each pixel in the eight-bit input image, the average (A) and the variance (V) from A of the data (D) over an 8×8 array of surrounding pixels is computed. The output image (O) is then obtained from the formula $O=(D-A)\{85/(V+17)\} + \frac{1}{2}A+64$. The first term has the effect of scaling up the corrugation in regions where the variance is small, while the second term reduces the effect of changes in average height, such as for steps. The formula given

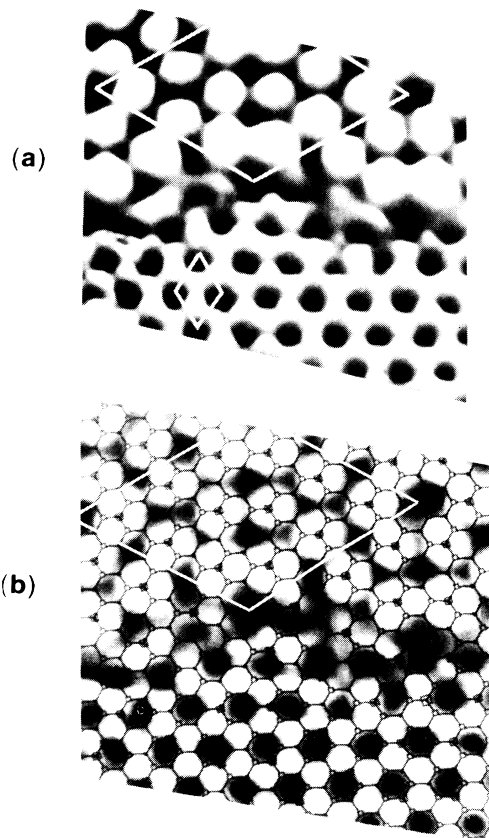


FIG. 2. STM image, with contrast enhancement, of a Si(111) 7×7 to Ag/Si(11) ($\sqrt{3}\times\sqrt{3}$) $R30^\circ$ domain boundary, recorded at $V_T=-2.0$ V and $i_T=2.0$ nA. (a) Three-dimensional view with 7×7 and $\sqrt{3}$ cell boundaries marked in white. Negative- V_T images are shown in all figures because they emphasize the adatom structure. Positive- V_T images in the same run establish that the right half of the 7×7 cell is faulted. (b) Top view with dark Si(111) mesh superimposed to show registration. White represents elevated features and small squares on the mesh mark adatom sites of the DAS model.

above represents default parameters of the image-processing programs employed¹² and was iterated twice to obtain the desired enhancement. The essential effect for the images in Figs. 2-4 is that the ratio of the corrugations for the $\sqrt{3}$ to those for the 7×7 structures is transformed from 0.1 to 0.4 so that both structures become readily visible. Three-dimensional perspective views of the processed data are provided for additional clarification. Finally, registration is obtained by use of a cursor to specify the Si adatom positions in an STM image together with corresponding adatom sites on a Si(111) mesh. The image processor then generates the transformation which best maps the Si adatom coordinates onto the DAS sites, using a least-squares fit, and overlays the image on the mesh.

Figure 2(a) shows a contrast-enhanced perspective view of a 7×7 to $\sqrt{3}$ transition, obtained with tip bias $V_T=-2.0$ V. The transition is extremely abrupt, with $\sqrt{3}$ regions extending into mildly perturbed 7×7 cells.

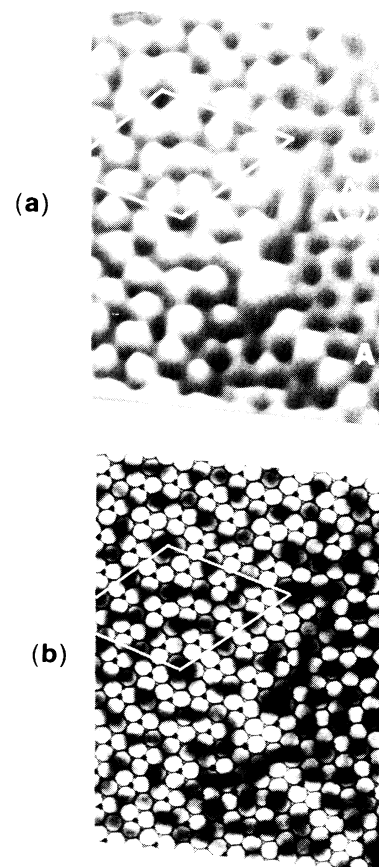


FIG. 3. Contrast-enhanced STM image, recorded at $V_T=-1.88$ V and $i_T=2.0$ nA, of a line of protrusions (A) in the lower right-hand corner which extends from the 7×7 onto the $\sqrt{3}$ domain. (a) Three-dimensional view with unit cells indicated. (b) Top view showing registration of $\sqrt{3}$ cells and of line defect features.

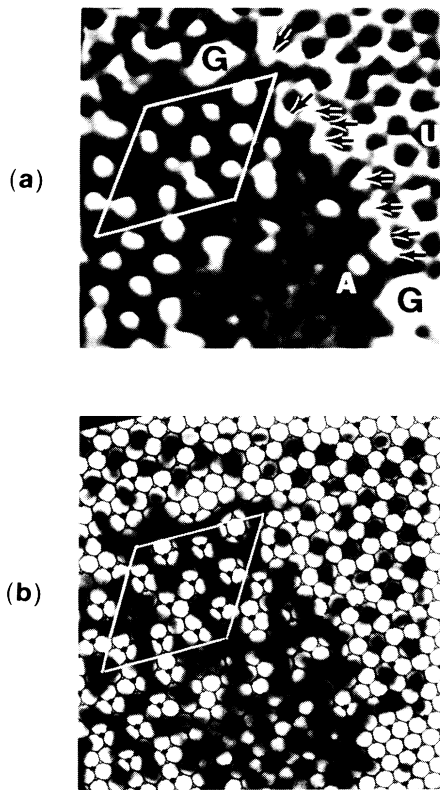


FIG. 4. STM image, with $V_T = -1.5$ V and $i_T = 2.0$ nA, after contrast enhancement which shows a step edge and domains of $\sqrt{3}$ and 7×7 structures. (a) Three-dimensional view with unit cells, globular defects (G), step edge features (arrows), and isolated adatoms (A) indicated. (b) Top view showing registration of these features.

The apparent height change between domains includes electronic structure effects and actually reverses, with the $\sqrt{3}$ structure appearing higher, if the tip bias voltage is lowered to -3.0 V. The gray-level image of Fig. 2(b) unambiguously demonstrates that the protrusions occur at the positions of Ag atoms in the H or MTL models. The images shown in Figs. 3 and 4, and other images recorded with positive V_T , confirm this result. The ET model of Refs. 3 and 4 is unequivocally ruled out.

In order to distinguish between the H and MTL models, additional information regarding the positions of surface Si atoms is needed. Figure 3(a) shows a domain boundary where a line of protrusions (A) extends from the 7×7 onto a region of $\sqrt{3}$ structure. The large height (2 \AA) and diameter (5 \AA) of these protrusions strongly resemble those of Si adatoms. Figure 3(b) shows that the registration of these features also coincides with that of Si adatoms on a complete double layer of Si. Note also that, in the H model, the top-layer Si atoms which are bonded to such adatoms do not belong to any of the adjacent $\sqrt{3}$ cells and would have the appropriate dan-

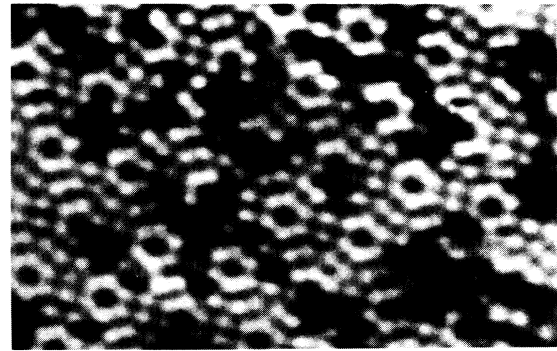


FIG. 5. STM image obtained, with $V_T = -2.7$ V and $i_T = 0.2$ nA, for nominal 0.25-monolayer Ag deposition on a room-temperature sample which was subsequently annealed to 480°C . Hexagonal corner holes of the 7×7 are evident.

gling bonds available for Si adatoms. If the top half of the Si double layer is missing, then these features register at an atop position. This is not expected for Si adatoms of for Ag atoms, which we have shown to occupy a hollow site. These features can, therefore, be easily understood as Si adatoms on the expected sites for the intact double-layer structure. For the MTL model they appear at sites not expected for either Ag or Si and cannot be readily explained.

Further information can be obtained by an examination of an image of a step edge, as shown in Fig. 4(a). The upper terrace (U) is composed entirely of $\sqrt{3}$ structure with two globular defects (G). This terrace steps down to $\sqrt{3}$ structure in one region and to 7×7 structure in another area. Right at the step edge are tall features, marked with arrows, which appear repeatedly along the step edge. Referring to Fig. 4(b), we find that these features appear to involve the top-layer site of the complete double layer of Si. We suggest that these features include a contribution from the charge density of top-layer Si atoms each of which has a broken bond associated with the step edge and a bond which is not shared between two adjacent $\sqrt{3}$ cells. If the top half of the Si double layer were missing, these sites presumably would be empty. Again we find a natural explanation of the STM step image provided the top double layer of Si is complete. The globular structures seen in this image are frequently observed at step edges and on the $\sqrt{3}$ terraces. We have observed similar structures in earlier work¹ where metal islands were expected since excess Ag was deposited and annealed to produce $\sqrt{3}$ structure. We find here that these features persist even at very low coverage. We speculate that these structures are associated with small Ag clusters and correspond to the initial appearance of the excess Ag discussed by Kono *et al.*⁵

Low-coverage Ag deposition onto room-temperature samples, subsequently annealed to 480°C , results in STM images exemplified by Fig. 5. The surface is dom-

inated by the 7×7 structure with extensive defects covering a fractional area corresponding roughly to the amount of silver deposited. We conclude that for room-temperature deposition Ag atoms do not diffuse sufficiently to form the island structures shown in Figs. 2–4. Even after annealing, the Ag atoms have diffused only a short distance before encountering enough Ag atoms, which appear to collectively destabilize Si adatoms, to allow an immobilizing reaction with the substrate to take place. This leads to an estimate for the critical nucleation size of about ten Ag atoms. For deposition on samples at 500°C , at nominal rates of 0.1 monolayer/min, Ag diffusion is fast enough that $\sqrt{3}$ domains form at steps and well-defined island growth occurs. STM has clear advantages for the understanding of nucleation phenomena, even prior to the formation of the intermediate layer.¹³

The data we have shown unambiguously demonstrate that the honeycomb features observed in STM are registered at threefold hollow sites of the Si(111) surface and can be associated with Ag atoms in the H or MTL models. The ET model is definitively ruled out. Images of steps and defects suggest further that the surface double layer of Si is intact so that the MTL model is unlikely. Although this evidence is less direct, it is strong compared to the photoemission data, which show rather little structure even for the 7×7 , that has been advanced to support the MTL model.⁵ It should be emphasized that STM has not, as yet, determined atomic identities through core-level or vibrational signatures. Rather, one is forced to rely on other techniques, such as coverage measurements,¹⁴ unless the electronic and geometric structure of the surface are known.¹⁵ For the Ag/Si(111) system, where the surface geometry is not established, we regard speculative electronic structure considerations as ambiguous, especially since electron-counting arguments give conflicting answers.^{3,5} Indeed, if the charge-transfer hypothesis of Kono is correct, then the electronic structure arguments used to interpret current-imaging tunneling spectroscopy data³ also favor a honeycomb Ag array. We cannot unequivocally rule out a trimer model where additional, but inequivalent,

Ag atoms reside in the honeycomb centers² or other models where severe distortions of the upper Si layers might match our registration results. However, given the excellent agreement of the honeycomb model with the registration of the STM images relative to the Si(111) mesh and with the results of other structural techniques,² we believe that the honeycomb model is correct.

The authors are deeply grateful for the invaluable assistance of M. Flickner and W. Niblack in the image processing.

¹R. J. Wilson and S. Chiang, Phys. Rev. Lett. **58**, 369 (1987).

²For a review of early work please see G. Le Lay, Surf. Sci. **132**, 169 (1983).

³E. J. van Loenen, J. D. Demuth, R. M. Tromp, and R. J. Hamers, Phys. Rev. Lett. **58**, 373 (1987).

⁴Y. Horio and A. Ichimiya, Surf. Sci. **164**, 589 (1985).

⁵S. Kono, K. Higashiyama, T. Kinoshita, T. Miyahara, H. Kato, H. Ohsawa, Y. Enta, F. Maeda, and Y. Yaegashi, Phys. Rev. Lett. **58**, 1555 (1987).

⁶S. Chiang and R. J. Wilson, IBM J. Res. Dev. **30**, 515 (1986).

⁷K. Takayanagi, Y. Tanishiro, S. Takahashi, and M. Takahashi, Surf. Sci. **164**, 367 (1985).

⁸G. Binnig, H. Rohrer, Ch. Gerber, and E. Weibel, Phys. Rev. Lett. **50**, 120 (1983).

⁹R. S. Becker, J. A. Golovchenko, E. G. McRae, and B. S. Swartzentruber, Phys. Rev. Lett. **55**, 2028 (1985).

¹⁰R. M. Tromp, R. J. Hamers, and J. E. Demuth, Phys. Rev. B **15**, 1388 (1986).

¹¹W. K. Pratt, *Digital Image Processing* (Wiley, New York, 1978).

¹²All images shown here were processed by IBM programs HLIPS and IAX on an IBM 4381 mainframe computer and displayed on an IBM 7350 display.

¹³M. Hanbücken, M. Futamoto, and J. A. Venables, Surf. Sci. **147**, 433 (1984).

¹⁴R. J. Wilson and S. Chiang, Phys. Rev. Lett. **58**, 2575 (1987).

¹⁵R. M. Feenstra, J. A. Stroscio, J. Tersoff, and A. P. Fein, Phys. Rev. Lett. **58**, 1192 (1987).

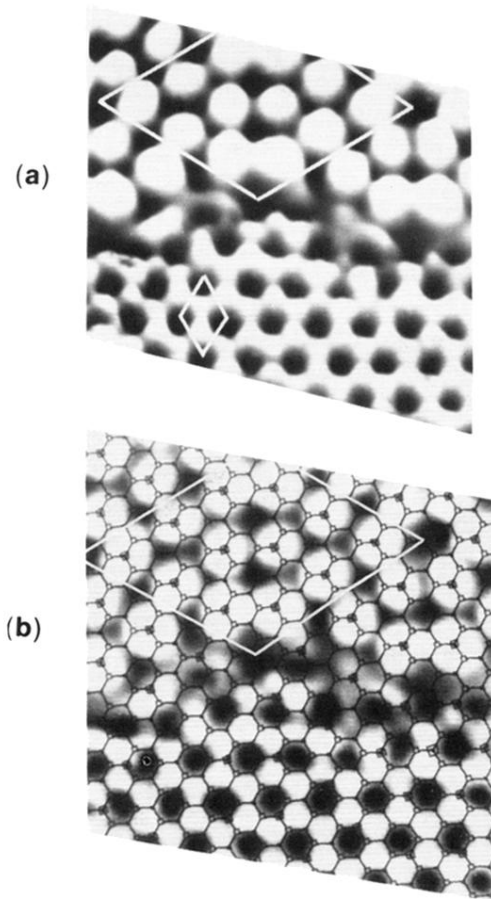


FIG. 2. STM image, with contrast enhancement, of a Si(111) 7×7 to Ag/Si(11) $(\sqrt{3} \times \sqrt{3})R30^\circ$ domain boundary, recorded at $V_T = -2.0$ V and $i_T = 2.0$ nA. (a) Three-dimensional view with 7×7 and $\sqrt{3}$ cell boundaries marked in white. Negative- V_T images are shown in all figures because they emphasize the adatom structure. Positive- V_T images in the same run establish that the right half of the 7×7 cell is faulted. (b) Top view with dark Si(111) mesh superimposed to show registration. White represents elevated features and small squares on the mesh mark adatom sites of the DAS model.

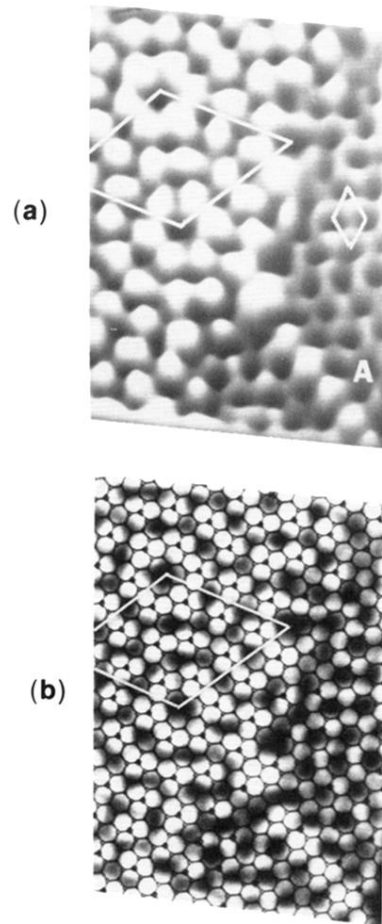


FIG. 3. Contrast-enhanced STM image, recorded at $V_T = -1.88$ V and $i_T = 2.0$ nA, of a line of protrusions (A) in the lower right-hand corner which extends from the 7×7 onto the $\sqrt{3}$ domain. (a) Three-dimensional view with unit cells indicated. (b) Top view showing registration of $\sqrt{3}$ cells and of line defect features.

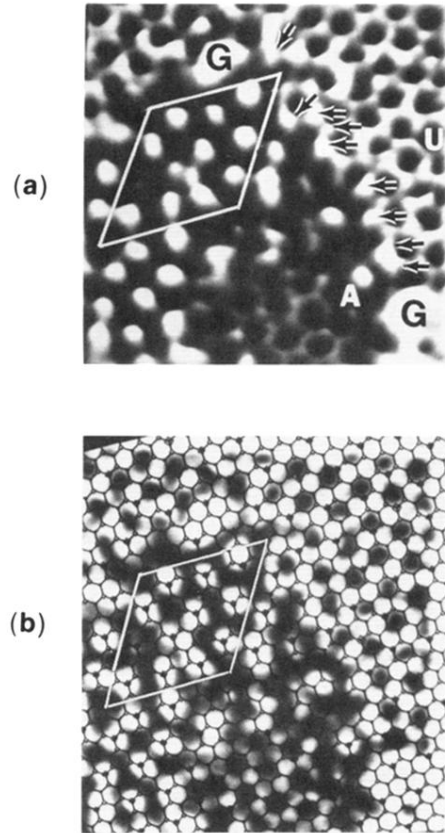


FIG. 4. STM image, with $V_T = -1.5$ V and $i_T = 2.0$ nA, after contrast enhancement which shows a step edge and domains of $\sqrt{3}$ and 7×7 structures. (a) Three-dimensional view with unit cells, globular defects (G), step edge features (arrows), and isolated adatoms (A) indicated. (b) Top view showing registration of these features.

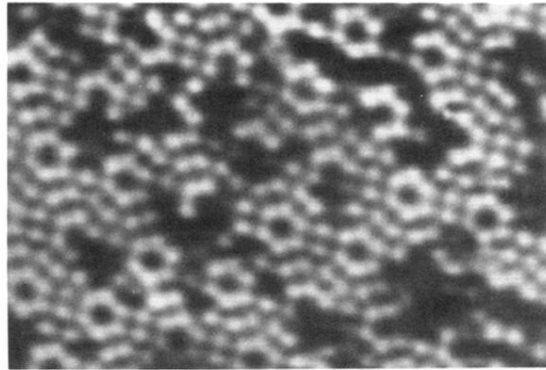


FIG. 5. STM image obtained, with $V_T = -2.7$ V and $i_T = 0.2$ nA, for nominal 0.25-monolayer Ag deposition on a room-temperature sample which was subsequently annealed to 480°C . Hexagonal corner holes of the 7×7 are evident.